Lung Cancer 98 (2016) 62–68

Contents lists available at ScienceDirect

Lung Cancer

journal homepage: www.elsevier.com/locate/lungcan

Spectral sensing for tissue diagnosis during lung biopsy procedures: The importance of an adequate internal reference and real-time feedback

Jarich W. Spliethoff[a,*], Lisanne L. de Boer[a], Mark A.J. Meier[b], Warner Prevoo[b], Jeroen de Jong[c], Torre M. Bydlon[f], Henricus J.C.M. Sterenborg[a,d], Jacobus A. Burgers[e], Benno H.W. Hendriks[f], Theodoor J.M. Ruers[a,g]

[a] Department of Surgery, Netherlands Cancer Institute, Plesmanlaan 121, 1066CX, Amsterdam, Netherlands
[b] Department of Radiology, Netherlands Cancer Institute, Plesmanlaan 121, 1066CX, Amsterdam, Netherlands
[c] Department of Pathology, Netherlands Cancer Institute, Plesmanlaan 121, 1066CX, Amsterdam, Netherlands
[d] Department of Biomedical Engineering and Physics, Academic Medical Centre, Meibergdreef 9, 1105AZ, Amsterdam, Netherlands
[e] Department of Thoracic Oncology, Netherlands Cancer Institute, Plesmanlaan 121, 1066CX, Amsterdam, Netherlands
[f] Minimally Invasive Healthcare Department, Philips Research, High Tech Campus 34, 5656AE, Eindhoven, Netherlands
[g] MIRA Institute, University of Twente, Building Zuidhorst, Room ZH 116, Enschede, Netherlands

ARTICLE INFO

Article history:
Received 15 February 2016
Received in revised form 17 May 2016
Accepted 25 May 2016

Keywords:
Lung cancer
Biopsy
Real-time guidance
Tissue diagnosis
Optical spectroscopy

ABSTRACT

Objectives: Difficulties in obtaining a representative tissue sample are a major obstacle in timely selecting the optimal treatment for patients with lung cancer or other malignancies. Having a modality to provide needle guidance and confirm the biopsy site selection could be of great clinical benefit, especially when small masses are targeted. The objective of this study was to evaluate whether diffuse reflectance spectroscopy (DRS) at the tip of a core biopsy needle can be used for biopsy site confirmation in real time, thereby enabling optimized biopsy acquisition and improving diagnostic capability.
Materials and methods: We included a total of 23 patients undergoing a routine computed tomography (CT) guided transthoracic needle biopsy of a lesion suspected for lung cancer or metastatic disease. DRS measurements were acquired during needle insertion and clinically relevant parameters were extracted from the spectral data along the needle paths. Histopathology results were compared with the DRS data at the final measurement position.
Results: Analysis of the collective data acquired from all enrolled subjects showed significant differences ($p < 0.01$) for blood content, stO_2, water content, and scattering amplitude. The identified spectral contrast matched the final pathology in 20 out of 22 clinical cases that could be used for analysis, which corresponds with an overall diagnostic performance of 91%. Three cases underlined the importance of adequate reference measurements and the need for real time diagnostic feedback. Continuous real time DRS measurements performed during a biopsy procedure in one patient provided clear information with respect to the variation in tissue and allowed identification of the tumour boundary.
Conclusions: The presented technology creates a basis for the design and clinical implementation of integrated fibre-optic tools for a variety of minimal invasive applications.

1. Introduction

Advances in molecular biology are improving the understanding of lung cancer and directing clinical decision making. Consequently, representative tissue samples for histologic characterization and mutation analysis are increasingly important. Furthermore, with the introduction of lung cancer screening programs [1–3] lung tumours are expected to be found at earlier stages when the lesions are smaller in size.

The modality selected for tissue diagnosis depends on multiple factors, including size, morphology, and – most important – location of the target lesion. For central pulmonary lesions the preferred method for tissue sampling is transbronchial needle aspiration (TBNA) via standard flexible bronchoscopy. TBNA may provide

Abbreviations: CT, computed tomography; DRS, diffuse reflectance spectroscopy; TBNA, transbronchial needle aspiration; FOBN, fibre-optic biopsy needle; GEE, generalized estimating equations; OCI, optical contrast index.

* Corresponding author.
E-mail address: j.spliethoff@nki.nl (J.W. Spliethoff).

http://dx.doi.org/10.1016/j.lungcan.2016.05.019
0169-5002/

diagnostic yields as high as 86% [4], but the yield strongly depends on the location and size of the pulmonary nodule. In case of small (<2 cm) lesions located in the periphery of the lung, the diagnostic yield is low (30–46%) [5–7].

Guidance by additional modalities such as endobronchial ultrasound or electromagnetic navigation may increase diagnostic performance, but diagnostic accuracy remains poor (56%) for small lesions [8,9]. For these peripheral lung nodules that are difficult to reach by bronchoscopy, percutaneous transthoracic fine needle aspirations or core needle biopsies are advocated. Although these procedures are generally performed under CT or fluoroscopy guidance, positioning the biopsy needle in or near small nodules remains challenging. As a consequence, the target lesion may be missed. Furthermore, biopsies may be inconclusive because non-diagnostic, necrotic material is obtained. Altogether, up to 23% [7,10–12] of the transthoracic diagnostic biopsy procedures for pulmonary lesions show fail, resulting in repeated biopsies and associated risk of pneumothorax and bleeding.

In recent years, promising achievements have been made in the field of diffuse reflectance spectroscopy (DRS). Diffuse Reflectance Spectroscopy (DRS) enables tissue characterization by illuminating the tissue with a selected spectral band of light and collecting diffusely reflected light. The light that is recollected has travelled through the tissue and contains information about the tissue's absorption and scattering properties. Analysis of this spectral signature provides specific quantitative morphologic, biochemical and functional information. We propose the use of a simple-to-use fibre-optic probe, which is integrated into biopsy needles that are commonly used for routine diagnostic purposes. Such a smart biopsy device would allow near real time measurement of tissue optical properties at the tip of the needle by DRS. This approach would allow rapid diagnosis *in vivo* and could therefore be used to increase the biopsy yield and prevent repeated biopsy procedures.

Our group previously validated a DRS spectroscopy platform that allows DRS tissue sensing at the tip of a biopsy needle with integrated optical fibres [13,14]. We demonstrated the value of the system by assessing its preliminary performance in a small number of patients undergoing transthoracic needle biopsy for suspicious lung lesions [15]. Tissue diagnosis derived from DRS was diagnostically discriminant in each of the 11 clinical cases that were investigated.

In the current study the performance of our method is investigated in a larger cohort of patients and a link is made between pooled results of the cohort data and the results based on an individual patient analysis. Furthermore, possible improvements for future clinical applicability were identified.

2. Materials and methods

2.1. Patients

The protocols for the clinical study were reviewed and approved by the institutional review board of The Netherlands Cancer Institute – Antoni van Leeuwenhoek hospital. The study was registered at the Netherlands Trial Register (NTR3651) and the U.S. National Institutes of Health Clinical Trial Database (NCT01730365). Patients with suspicious pulmonary lesions who were scheduled for a standard core needle biopsy were recruited for study participation. The lesions had to be safely accessible by a transthoracic core biopsy needle. The lesions were required to be located in the pulmonary parenchyma at least 1 cm from the pleural surface to allow reference measurements in lung parenchyma. Patients at increased risk of bleeding were excluded. All patients gave written informed consent prior to the experimental procedures.

2.2. Portable spectroscopy system

The general principles of DRS, the operating features of the DRS system, the calibration procedures, and fibre-optic biopsy needle (FOBN) have been described previously [16,17]. Briefly, the 16G FOBN (Invivo Germany, Schwerin, Germany) consists of one 100 μm diameter fibre for light delivery and two identical adjacent fibres with a diameter of 200 μm for the collection of the reflected light. The distance between the emitting and collecting fibres at the needle tip was 1.36 mm, resulting in a tissue probing depth of approximately 1–2 mm. The optical fibres from the FOBN were connected to the DRS system, which consists of a broad-band light source (Tungsten halogen; 360–2500 nm) and two spectrometers: one which resolves the light in the visible wavelength range, *i.e.* 400 up to 1050 nm (Andor Technology, DU420A-BRDD) and one which resolves near infrared light from 900 up to 1700 nm (Andor Technology, DU492A-1.7). For each procedure the system was calibrated for system response by measuring reflectance from a spectrally flat barium sulphate casing around a non-sterile calibration needle. This permitted correction for spectral variations of the light source, spectrometer, and fibre transmission. After the calibration, the calibration needle was disconnected and the sterile-packaged experimental needle was connected.

2.3. Image guidance and data acquisition

All patients underwent a free-breathing CT-scan (16-slice Somatom Sensation Open, Siemens, Erlangen, Germany) as part of the standard procedure planning. From the 3D data set, an optimal slice with the tumour clearly visible was selected to define a planned needle path. The fibre-optic biopsy needle was inserted at the planned entry point and fluoroscopy imaging was performed simultaneously with DRS acquisition to allow registration of the tissue characterization with the actual location of the needle tip. A total of 23 patients were measured. In 22 patients sets of 3–5 reflectance spectra were acquired at discrete locations in 1) healthy lung tissue, 2) tissue at the tumour border, and 3) tumour tissue. In one patient DRS measurements were taken in rapid succession (within ~1.5 s) along the needle tract. For each patient the biopsy gun was fired immediately after final DRS measurements to obtain a physical tissue sample from the target lesion.

2.4. Tissue processing

The distal end of the tissue samples was marked with yellow tissue marking dye (Polysciences Inc., Warrington, United Kingdom) for orientation purposes. The samples were formalin-fixed and processed according to routine histopathology. Tissue samples were processed via standard histological procedures. After paraffin embedding, the samples were sectioned and stained with standard hematoxylin and eosin (H&E) (Merck, Darmstadt, Germany). The resulting tissue slices were examined by light microscopy by an experienced pathologist who was blinded to the spectroscopic findings. The glass slides were digitized by a histologic slide scanner (ScanScope – Aperio Technologies Inc., Vista, California). Pathology results were compared with the DRS data at the final measurement position.

2.5. Spectral data analysis

DRS measurements were spectrally fitted with an analytical model by Farrell et al. [18] that was derived from diffusion theory using a Levenberg–Marquardt non-linear inversion algorithm to determine the absorption coefficient $\mu_a(\lambda)$ and the reduced scattering coefficient $\mu_s(\lambda)$ expressed in cm^{-1}. The validation of the model, including spectral calibration procedures, and its application in

various preclinical studies were described in detail elsewhere [13,14,19,20].

The model uses prior knowledge of light-tissue interaction to translate the acquired spectra into estimates of various absorption and scattering parameters. The absorption parameters represent the concentration of physiologically relevant absorbers in the tissue (*e.g.* blood, water, fat) as well as functional parameters like the oxygenation level of blood [stO_2]. The absorption coefficient of water and fat in their pure state is used as a priori knowledge for the model-based analysis. The blood content is computed as the sum of the estimated oxygenated and deoxygenated haemoglobin volume fraction by assuming a total haemoglobin concentration of 150 mg/mL of blood (typical value for human blood). The oxygenation level of blood is computed as the ratio of oxygenated haemoglobin to the total blood volume fraction. Light scattering is caused by local inhomogeneity in the refractive index, such as cellular organelles and extracellular matrix [21,22] or in lung by air-tissue transitions in alveoli. In lung, the main scattering parameter is the reduced scattering amplitude, which we calculated at 800 nm [$\mu_s'(800)$].

2.6. Outcome measures and statistics

Tissue parameters determined from DRS spectral measurements (*e.g.* blood, stO_2, water, $\mu_s'(800)$) were compared between tumour tissue and normal tissue using a generalized estimating equations (GEEs) approach with controlling for repeated measurements within the same subject. These DRS parameters were assumed to be normally distributed. Within-patient dependencies were represented by the correlation matrix where all pairwise correlations were assumed to be equal (equicorrelated). The analyses were performed using the GEEQBOX toolbox in Matlab 8.4 (MathWorks Inc., Natick, Massachusetts) and $p < 0.01$ were considered statistically significant.

Earlier we found that when performing pooled analysis of all spectra, DRS parameters may show considerable overlap between various tissue types due to inter-patient variation. Moreover, to allow incorporation of multiple optical fibres in a thin biopsy needle, we used a fibre separation of 1.36 mm, which – in some cases – will infringe with diffusion theory assumptions, resulting in an overestimation of absorption coefficients and scattering parameters. An approach to overcome these issues is to focus on relative changes that occur in a particular insertion instead of looking at absolute values only [15,23,24].

To compare the results of the pooled analysis and individual patient data, parameter values for blood content, stO_2, water content, and $\mu_s'(800)$ were scaled to the average values measured within each patient. Furthermore, for each patient an Optical Contrast Index (OCI) was calculated, which represents the relative difference in the water-to-scattering ratio between tumour and lung tissue within the same individual [15]. OCI values were determined based on the spectroscopically derived values for water and $\mu_s'(800)$ using the following formula:

$$OCI = \frac{\left[\text{water}/\mu_s'(800)\right]_{\text{Tumor}}}{\left[\text{water}/\mu_s'(800)\right]_{\text{Normal}}},$$

where $\left[\text{water}/\mu_s'(800)\right]_{\text{Tumor}}$ and $\left[\text{water}/\mu_s'(800)\right]_{\text{Normal}}$ correspond to the average water-to-scattering ratio measured in tumour tissue and surrounding normal lung tissue, respectively.

3. Results

Twenty-three transthoracic biopsy procedures were performed using the experimental device. Median age was 67 years (range 41–80 years). Twelve participants were women, 13 were smokers. Histopathological examination of the targeted tissue revealed 21 malignancies and one hamartoma (Table 1). One tissue sample was non-diagnostic. The median tumour size was 27 mm (range 12–63 mm).

Table 1
Histopathology findings and lesion size for the 23 suspicious lung lesions.

Lesion	Clinical diagnosis	*n*	Median lesion size in mm
Malignant tumour ($n = 21$)	Non-small-cell lung carcinoma	17	29 (range 14–63)
	Metastasis of a colon carcinoma	2	30 (range 12–47)
	Metastasis of a carcinoma of the ovary	1	14
	Metastasis pleiomorf sarcoma	1	32
Benign tumour ($n = 1$)	Hamartoma	1	20
Non-diagnostic ($n = 1$)	Lung parenchyma	1	18
Total		23	27

During needle insertion, positioning of the FOBN in lung parenchyma was based on the CT fluoroscopy imaging, as illustrated in Fig. 1. When the collective data (n = 242 DRS spectra) acquired from all enrolled subjects were statistically compared (Fig. 2A), significant compositional differences ($p < 0.01$) between tumour tissue and surrounding healthy lung tissue were noted for stO_2, water content, and $\mu_s'(800)$. On average more blood was encountered during measurements in healthy lung tissue, but this difference was not statistically significant.

Fig. 2B shows the relative contrast between tumour and normal tissue based on the spectroscopically derived values for blood content, stO_2, water content, and $\mu_s'(800)$ for each patient individually. Note that for stO_2, water content, and $\mu_s'(800)$ the trends from lung parenchyma to tumour tissue showed the same tendency for most patients (down for stO_2 and $\mu_s'(800)$; up for water content). Additionally, in most patients more blood was encountered in healthy lung parenchyma, but considerable differences between patients was seen.

Comparison of the DRS OCI values with the biopsy reports showed that in 19 out of 23 patients, tumour tissue could be correctly identified based on a median increase in the OCI of 131%. In four cases the OCI did not increase during the biopsy procedure. One of these cases (*subject* 3) appeared to be a "true-negative"; the OCI (0.72) measured just before biopsy indicated that FOBN was not positioned in or near the lesion. Histopathological analysis of the biopsy sample confirmed that the targeted lesion was missed. Thus if this feedback would have been used, a corrective manipulation of the needle may have increased the chance of an adequate biopsy.

As mentioned previously, the integrated fibre-optic biopsy tool used for the spectral measurements enables 1:1 correlation between spectral data and the tissue sample taken at the same location in the tumour. However, in one patient (*subject 18*), during the procedure the fluoroscopic imaging showed that the needle was slightly moved between the final spectral measurements and the actual tissue biopsy. This resulted in a mismatch between the OCI value (0.94) and pathology analysis. This observation highlights the importance of real time measurements and data processing in order to allow for necessary adjustments of needle positioning based on the changes in the derived DRS parameters.

Furthermore, we found that in two patients (Fig. 3: *subject 16* and *subject 19*) inadequate reference measurements in normal lung parenchyma led to impaired lesion identification when using the OCI (values: 0.68 and 0.81 for subject 16 and subject 19, respectively) as end point. The fluoroscopic imaging of *subject 16* (Fig. 3A)

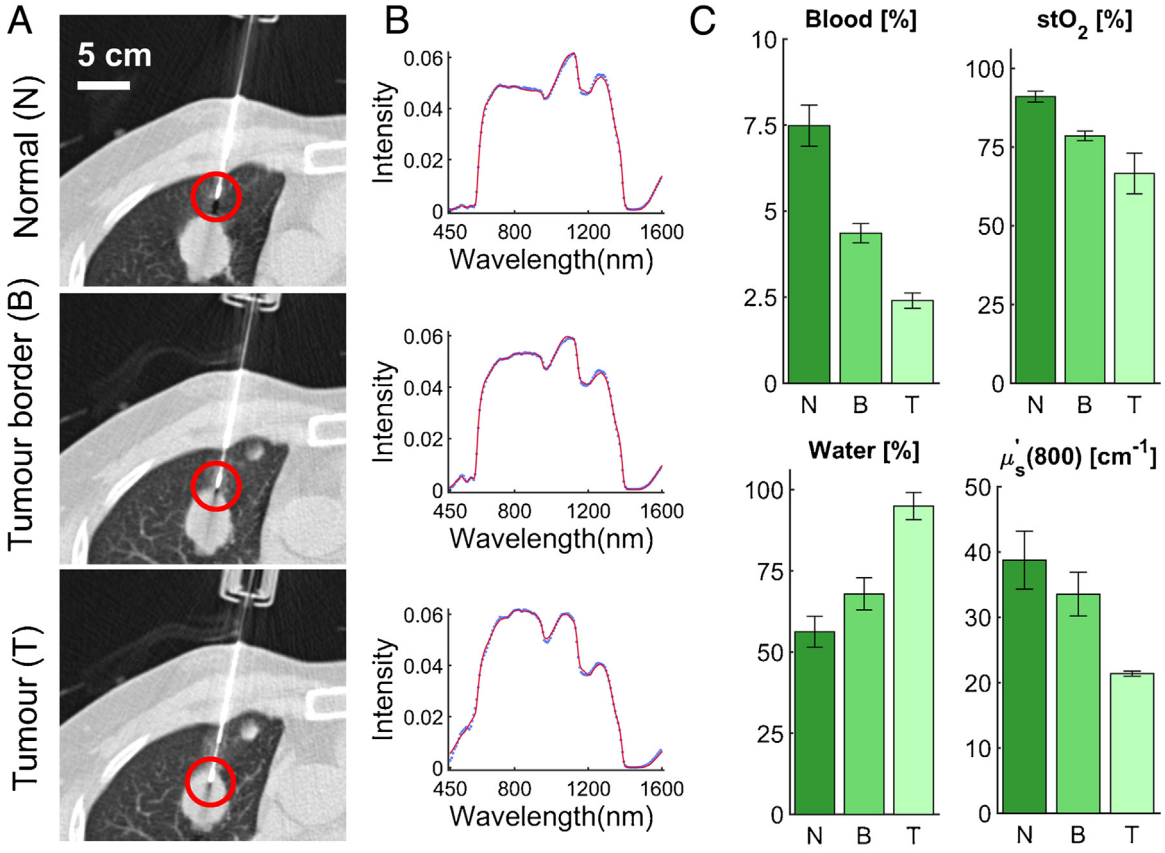

Fig. 1. Example of added quantitative spectral functionality during routine lung biopsy. (A) Positioning of the FOBN based on CT fluoroscopy imaging in lung tissue, near the target lesion and in the target lesion prior to biopsy. (B) Co-registered DRS measurements (blue dotted line) and corresponding fit curves (red lines). (C) Data for blood, stO2, water and μs'(800) represent mean values ± standard error of the mean. N: normal lung parenchyma; B: tumour border; T: tumour.

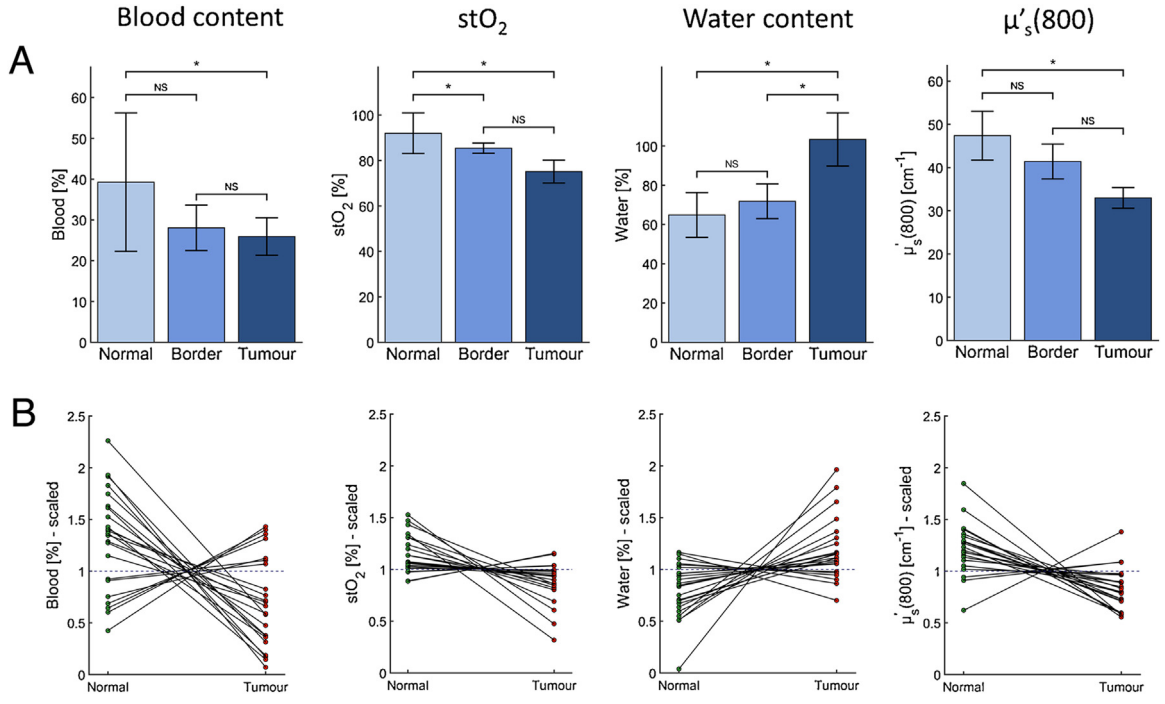

Fig. 2. DRS parameter quantification. (A) Bar graphs showing the values for blood, stO2, water, and μs'(800) as measured in lung parenchyma (Normal), at the tumour border (Border) and in the target lesion (Tumor). Values are given as the mean ± standard error, adjusted for repeated measurements. *$p < 0.01$. NS: not significant. (B) Relative differences in blood, stO2, water, and μs'(800) between lung parenchyma and tumour for individual needle insertions ($n = 22$).

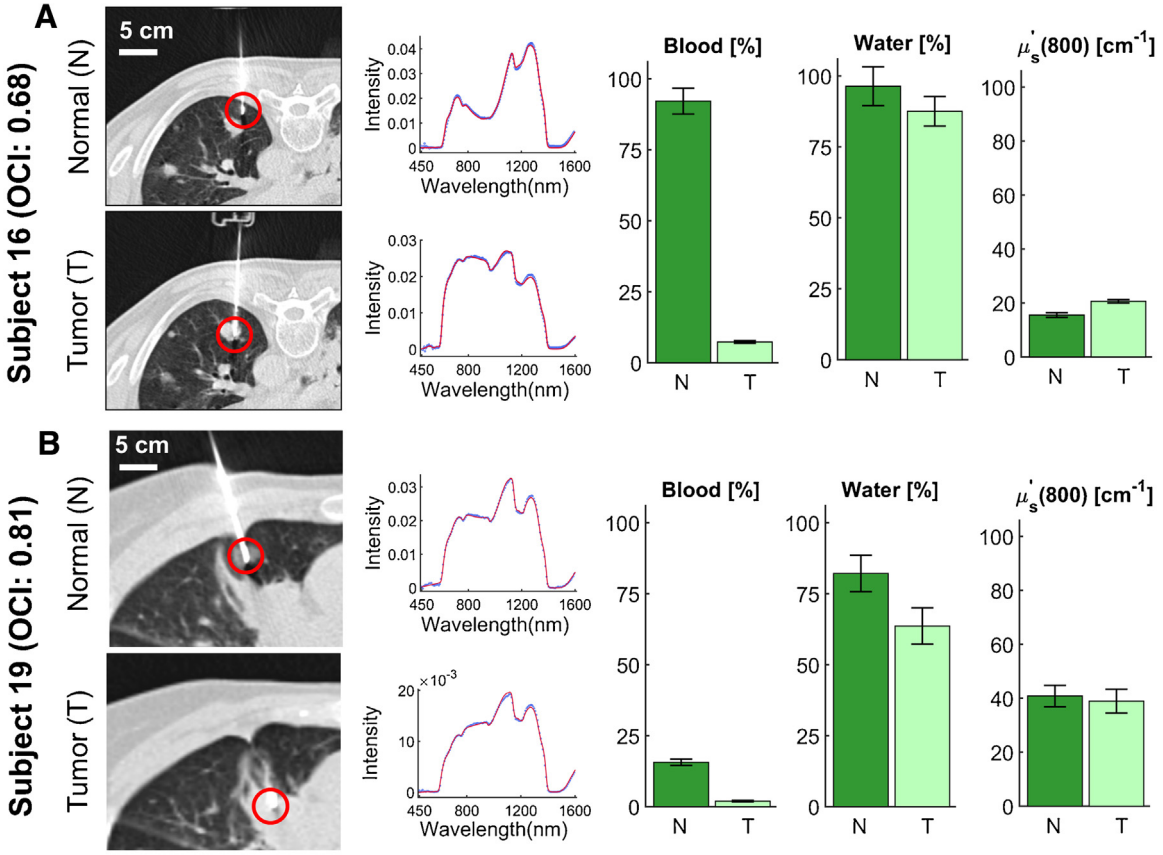

Fig. 3. (A) Fluoroscopic imaging of subject 16 confirms that reference measurements were taken in lung parenchyma. However, these measurements appeared to contain 92% blood. (B) In subject 19 fluoroscopic imaging suggests that reference measurements were not taken in healthy lung parenchyma. Both clinical cases underline the importance of adequate reference measurements. N: normal lung parenchyma; T: tumour.

suggested that DRS reference measurements were taken in healthy lung parenchyma. However, based on DRS blood content (>90%) these measurements might have been taken near a small blood vessel or minor bleeding at the needle tip. In *subject 19* (Fig. 3B) fluoroscopic imaging indicated that reference measurements were not taken in healthy lung parenchyma, but in consolidated tissue. What is important to note, is that in both clinical cases either spectral information (measured blood content) or procedural fluoroscopy imaging could have been used to inform the operator about the (in)adequacy of the reference measurements.

In one patients (subjects 23) spectral measurements were acquired continuously during needle insertion, as shown in Fig. 4. While the needle tip was progressed towards the tumour, CT fluoroscopy imaging provided the actual location of the needle tip. A clear increase in OCI was observed once the needle reached the tumour, indicating that this information could have been used to verify correct needle positioning.

4. Discussion

In the current study, we sought to assess the potential of DRS as a platform for the real time lesion identification during routine transthoracic core-needle biopsy procedures. We believe that feasibility and usability have been demonstrated successfully.

A total of 23 transthoracic lung needle biopsies performed under fluoroscopy imaging. Tissue water content, stO_2, and $\mu_s'(800)$ showed statistically significant differences when the needle tip was guided from normal lung tissue to the target lesions. These findings are in line with our previous studies [13–15]. Relative differences in water-to-scattering ratio matched with final pathology in 20 out of 22 clinical cases that could be used for analysis. This corresponds with an overall diagnostic performance of 91%. Two clinical cases underlined that a robust internal reference measurement is needed for accurate detection of transitional changes along the needle track. Furthermore, we learned that the diagnostic spectral information should be presented in real time to minimize discrepancies between DRS measurements and the actual biopsy site due to needle movement.

The key advantage of our system is that is that the narrow wavelength range commonly used in DRS (typically between 400 and 900 nm) was extended into the near-infrared region up to 1600 nm where blood has no significant absorption features. This feature helps to overcome the effect of dominant absorption by excessive amounts of haemoglobin in the visible wavelength region (400–700 nm). Furthermore, it enables the quantification of water content which is an important measure for lung tissue density. Earlier, we found that the reliability (*i.e.* confidence intervals) for water content and $\mu_s'(800)$ is not affected by the amount of blood at the needle tip. However, in case of excessive pooling of blood at the needle tip, DRS output parameters might not reflect the tissue's true physiological composition. Thus, although the estimates for the DRS parameter values may be valid, the parameter values may partly reflect the optical properties of blood. Nevertheless, the blood content –which is accurately quantified- could be provided as feedback to the physician, thereby allowing necessary adjustments of the needle to reduce the effect of blood contamination.

From a clinical point of view, a system for spectral tissue sensing should provide clear contrast between the target tissue (tumour) and surrounding tissue. Continuous DRS measurements, as performed during this study, can be used to record a profile along the

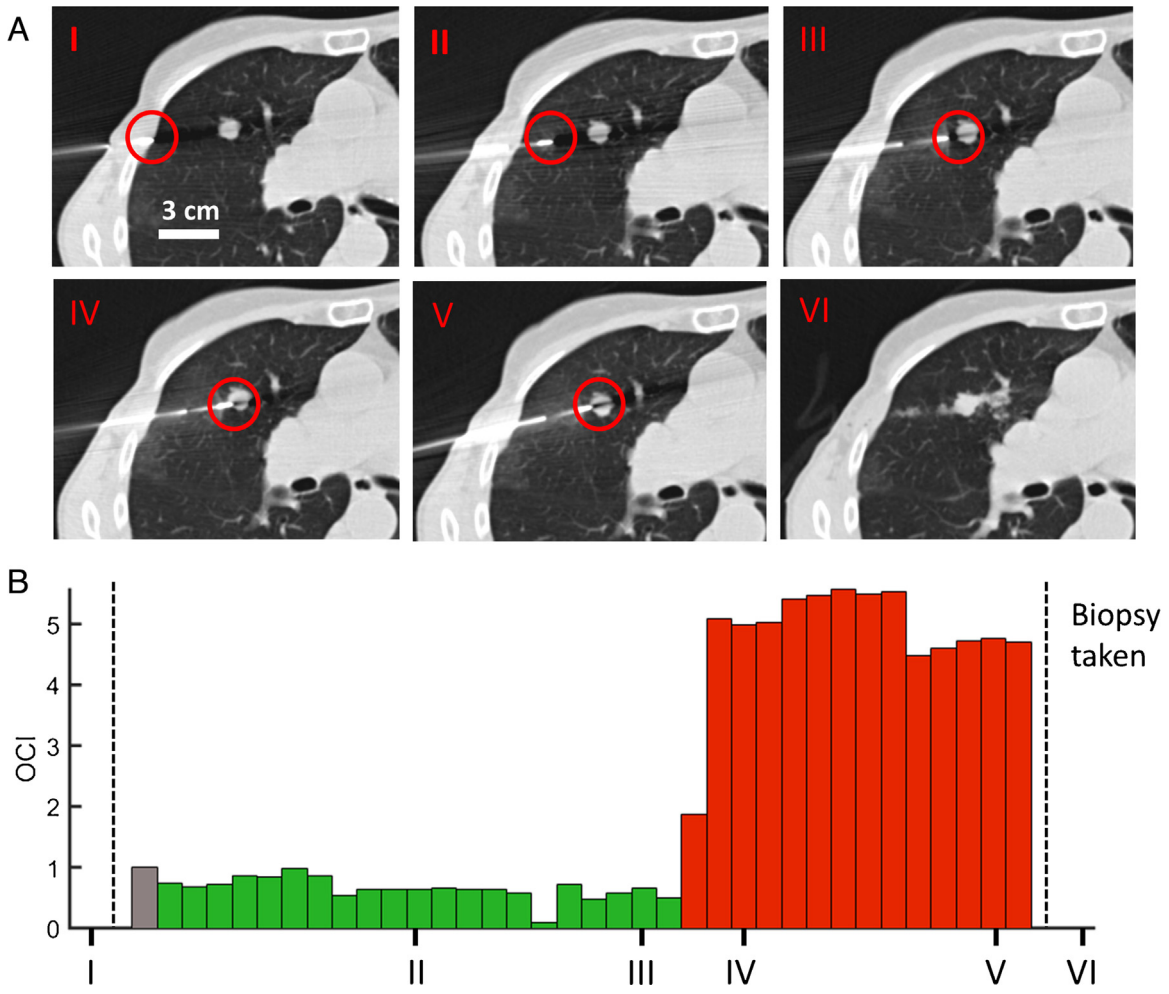

Fig. 4. Real time tissue characterization and biopsy with the FOBN in an individual. (A) CT Fluoroscopy images during insertion of the FOBN (images I through V) and after the biopsy has been performed (image VI). (B) The OCI was extracted from the optical data along the needle path. Note that the first measurement in lung parenchyma served as internal reference.

needle path and yield valuable data with respect to the variation in tissue composition across the tumour as well as identifying the boundaries between tissues. However, from the results of this study we learned that spectral tissue feedback should preferably also include information about the reliability of the spectral measurement and the certainty of an assigned tissue diagnosis. A strategy using a combination of multiple DRS parameters (including blood content) and corresponding confidence intervals may have the potential to improve the overall reliability of a future clinical application.

We should note that using healthy lung tissue as reference is only applicable to lesions with sufficient aerated lung parenchyma interposed between the pleura the lesion. Lesions located close to the pleura or lesions that are obscured by fibrosis or atelectasis are not amenable for this method. One option is to perform a reference measurement in subcutaneous fat at the skin entry site prior to further needle insertion into the thorax. These measurements could then be used to correct for inter-patient variation. Additional advantages would be the simplification of the biopsy process and decreased risk of complications, specifically pneumothorax or hemorrhage, as spectral reference measurements are taken prior to piercing the pleura.

The calibration of the spectroscopy system prior to tissue measurements consisted of several steps, including calibrating the system with a white reflectance standard measurement to correct for system response (spectral variations of the light source, spectrometer, fibre transmission, *etc.*). For the *in vivo* studies the spectroscopy system was calibrated for system response by measuring reflectance from a spectrally flat barium sulphate casing around a non-sterile calibration needle. After the calibration, the calibration needle was disconnected and the sterile-packaged fibre-optic needle was connected for the tissue measurements. Although this method allows correcting for day-to-day variations, it does not take into account differences between the single-use fibre-optic needles and variations in the coupling between the fibre-optic needles and the spectroscopy system. It would be interesting to investigate the contribution of this source of error to the "inter-patient" variation. For a future clinical system one could consider packaging the spectroscopy needle with a calibration cap in place. This cap could then be used for system calibration (after connection of the needle) without contaminating the needle.

Because STS is performed from tissues that are close to the needle tip (1–2 mm), we expect that spectral information will ultimately be used complementary to image guidance *(e.g.*, fluoroscopic imaging). By providing crucial information just before the tissue sample is taken STS may help to reduce the number of false-negative biopsies with minimal impact on routine clinical workflow.

The current experimental system was designed for clinical studies and has proven to be compatible with the existing clinical workflow of transthoracic lung biopsy procedures. Because of the observational nature of this study, the collected data were not

shown to the radiologist. Further clinical validation of the outlined approach in a prospective setting or (subsequent) clinical implementation would require that the spectral information is translated into comprehensible and reliable diagnostic information in real time.

Precise biopsy needle placement and positioning will remain the basis of every successful biopsy procedure. CT-guided core needle biopsy is viewed as a safe procedure for diagnosing pulmonary nodules, but accuracy decreases with a smaller lesion size, making definitive diagnosis difficult. Conventional CT-guided needle biopsies of the lung do not allow real time visualization of the needle tip or the site of the lesion. This lack of real time imaging capability is one reason for a decrease in diagnostic accuracy [25]. We expect that once optimized, the combined use of image guidance and real time spectral tissue characterization may improve the diagnostic performance of transthoracic biopsies of small peripheral lung lesions to 90–95%. This objective should be challenged in a larger prospective diagnostic study.

5. Conclusions

We conclude that DRS tissue sensing integrated into a biopsy needle may be a powerful new tool for biopsy guidance that can be readily used in routine diagnostic lung biopsy procedures. Given the feasibility and clinical applicability of the outlined approach, it is also conceivable to make integrated tools for other oncological procedures that rely on accurate instrument positioning.

Disclosure

Technical support for this study was provided by Philips research, Eindhoven, the Netherlands. The authors declare no competing financial interests.

Acknowledgements

We thank J.J.J. de Vries, M. Müller, V.V. Pully, C. Reich and M. van der Voort for their assistance in conducting the clinical experiments; N. Langhout for helpful discussion on the experimental results; and E. Kho for attentive reading of the manuscript.

References

[1] D.R. Aberle, C.D. Berg, W.C. Black, et al., The national lung screening trial: overview and study design, Radiology 258 (2011) 243–253.
[2] M. Oudkerk, M.A. Heuvelmans, Screening for lung cancer by imaging: the Nelson study, JBR-BTR 96 (2013) 163–166.
[3] The national lung screening trial research, T. results of initial low-dose computed tomographic screening for lung cancer, N. Eng. J. Med. 368 (2013) 1980–1991.
[4] J.S. Wang Memoli, P.J. Nietert, G.A. Silvestri, Meta-analysis of guided bronchoscopy for the evaluation of the pulmonary nodule, Chest 142 (2012) 385–393.
[5] M.K. Gould, J. Fletcher, M.D. Iannettoni, et al., Evaluation of patients with pulmonary nodules: when is it lung cancer?: ACCP evidence-based clinical practice guidelines (2nd edition), Chest 132 (2007) 108s–130s.
[6] R. Eberhardt, A. Ernst, F.J. Herth, Ultrasound-guided transbronchial biopsy of solitary pulmonary nodules less than 20 mm, Eur. Respir. J. 34 (2009) 1284–1287.
[7] M.P. Rivera, F. Detterbeck, A.C. Mehta, Diagnosis of lung cancer: the guidelines, Chest 123 (2003) 129s–136s.
[8] D.P. Steinfort, Y.H. Khor, R.L. Manser, et al., Radial probe endobronchial ultrasound for the diagnosis of peripheral lung cancer: systematic review and meta-analysis, Eur. Respir. J. 37 (2011) 902–910.
[9] L.M. Ofiara, A. Navasakulpong, N. Ezer, et al., The importance of a satisfactory biopsy for the diagnosis of lung cancer in the era of personalized treatment, Curr. Oncol. 19 (2012) S16–S23.
[10] N. Kothary, L. Lock, D.Y. Sze, et al., Computed tomography-guided percutaneous needle biopsy of pulmonary nodules: impact of nodule size on diagnostic accuracy, Clin. Lung Cancer 10 (2009) 360–363.
[11] Y. Gong, N. Sneige, M. Guo, et al., Transthoracic fine-needle aspiration vs concurrent core needle biopsy in diagnosis of intrathoracic lesions: a retrospective comparison of diagnostic accuracy, Am. J. Clin. Pathol. 125 (2006) 438–444.
[12] A.M. Priola, S.M. Priola, A. Cataldi, et al., CT-guided percutaneous transthoracic biopsy in the diagnosis of mediastinal masses: evaluation of 73 procedures, Radiol. Med. 113 (2008) 3–15.
[13] D.J. Evers, R. Nachabe, H.M. Klomp, et al., Diffuse reflectance spectroscopy: a new guidance tool for improvement of biopsy procedures in lung malignancies, Clin. Lung Cancer 13 (2012) 424–431.
[14] J.W. Spliethoff, D.J. Evers, H.M. Klomp, et al., Improved identification of peripheral lung tumors by using diffuse reflectance and fluorescence spectroscopy, Lung Cancer 80 (2013) 165–171.
[15] J.W. Spliethoff, W. Prevoo, M.A. Meier, et al., Real-time in vivo tissue characterization with diffuse reflectance spectroscopy during transthoracic lung biopsy: a clinical feasibility study, Clin. Cancer. Res. 22 (2016) 273–274.
[16] R. Nachabe, B.H. Hendriks, M. van der Voort, et al., Estimation of biological chromophores using diffuse optical spectroscopy: benefit of extending the UV–vis wavelength range to include 1000–1600 nm, Biomed. Opt. Express 1 (2010) 1432–1442.
[17] R. Nachabe, B.H. Hendriks, A.E. Desjardins, et al., Estimation of lipid and water concentrations in scattering media with diffuse optical spectroscopy from 900 to 1,600 nm, J. Biomed. Opt. 15 (2010) 037015.
[18] T.J. Farrell, M.S. Patterson, B. Wilson, A diffusion theory model of spatially resolved, steady-state diffuse reflectance for the noninvasive determination of tissue optical properties in vivo, Med. Phys. 19 (1992) 879–888.
[19] D.J. Evers, R. Nachabe, M.J. Vranken Peeters, et al., Diffuse reflectance spectroscopy: towards clinical application in breast cancer, Breast Cancer Res. Treat. 137 (2013) 155–165.
[20] D.J. Evers, R. Nachabe, D. Hompes, et al., Optical sensing for tumor detection in the liver, Eur. J. Surg. Oncol. 39 (2013) 68–75.
[21] G. Zonios, A. Dimou, Light scattering spectroscopy of human skin in vivo, Opt. Express 17 (2009) 1256–1267.
[22] O.C. Marina, C.K. Sanders, J.R. Mourant, Correlating light scattering with internal cellular structures, Biomed. Opt. Express 3 (2012) 296–312.
[23] P. Taroni, A. Pifferi, G. Quarto, et al., Effects of tissue heterogeneity on the optical estimate of breast density, Biomed. Opt. Express 3 (10) (2012) 2411–2418.
[24] A.M. Laughney, V. Krishnaswamy, E.J. Rizzo, et al., Scatter spectroscopic imaging distinguishes between breast pathologies in tissues relevant to surgical margin assessment, Clin. Cancer Res. 18 (22) (2012) 6315–6325.
[25] H. Tsukada, T. Satou, A. Iwashima, et al., Diagnostic accuracy of CT-guided automated needle biopsy of lung nodules, Am. J. Roentgenol. 175 (2000) 239–243.